



# Synthesis and cell uptake of a novel dualmodality $^{188}\text{Re}$ -HGRGD (D) F-CdTe QDs probe

Zheng Li, Guoxin Zhang, Hua Shen, Lan Zhang, Yongxian Wang\*

Radiopharmaceutical Centre, Shanghai Institute of Applied Physics, Chinese Academy of Sciences, 2019 Jia Luo Road, Shanghai 201800, China

## ARTICLE INFO

### Article history:

Received 17 December 2010

Received in revised form 22 April 2011

Accepted 29 April 2011

Available online 6 May 2011

### Keywords:

Quantum dots

$^{188}\text{Re}$

Dualmodality probe

Cell binding

## ABSTRACT

A novel dualmodality probe was prepared by linking  $^{188}\text{Re}$ -HGRGD (D) F with CdTe QDs, which was monitored using radio-thin layer chromatography (TLC) and -high performance liquid chromatography (HPLC). The  $^{188}\text{Re}$ -HGRGD (D) F-CdTe QDs probe possesses a radiochemistry yield of 92.1% and strong photoluminescence (PL) stability. However, the radiochemical purity of  $^{188}\text{Re}$ -HGRGD (D) F-QDs would reduce to 74.8%, which should be further improved, after incubation with newborn calf serum (NCF) for 24 h. Human glioblastoma U87MG cells, known to express a high-affinity to RGD, were used to assess the *in vitro* cell binding of probe. The results showed that the radio-signal was in accord with the change of PL intensity, which meant the successful integration of  $^{188}\text{Re}$  and QDs.

Crown Copyright © 2011 Published by Elsevier B.V. All rights reserved.

## 1. Introduction

CdTe quantum dots (QDs) have attracted numerous investigations because of its high quantum yield (QY), multicolor availability and functionality [1–3]. They usually possess broad excitation spectra, narrow emission bandwidth, broad Stokes shift and reduced tendency to photobleach compared with organic dyes [4,5]. So, they have been used as fluorescent probes for biological imaging widely. However, they are usually challenging *in vivo* owing to strong background autofluorescence and absorption or scattering of optical photons [6]. In addition, it is difficult to effectively quantify QD signal in living subjects according to fluorescence intensity alone, particularly in deep tissues, due to the current obstacles in fluorescence tomography [7,8]. So, the multifunctional QD-based probes for multimodality molecular imaging *in vitro* and *in vivo* have been developed to obtain enough necessary information for further research.

An Anx5-QD-Gd nanoparticle was presented to exhibit intense fluorescence and a large magnetic resonance relaxivity due to a newly designed construction increasing the gadolinium-DTPA load. It could analyze biological samples as well as vascular structures with MRI at the anatomical level and with TPLSM at the cellular level [9]. Furthermore, a series of core/shell CdSe/Zn<sub>1-x</sub>Mn<sub>x</sub>S nanoparticles were synthesized for use in dual-mode optical and MRI techniques, too [10]. Except for multifunctional QD-based probes with optical and MR imaging, a few other reports have

focused on radiolabeling QDs with PET isotopes to prepare PET/NIRF imaging probe. Polymer- or peptide-coated  $^{64}\text{Cu}$ -labeled QDs were used to evaluate the quantitative biodistribution of QDs in mice [11,12]. Furthermore, the  $^{18}\text{F}$ -labeling PEG-phospholipid QD micelles would make the best of two in *in vivo* molecular imaging systems: PET imaging for whole body imaging and fluorescence imaging for subcellular localization [13]. The development of dual-modality QDs-based imaging probes will allow for sensitive, accurate assessment of the tumor-targeting efficacy due to they would offer a quantitative analysis of the biodistribution of QDs-based probes and it would greatly facilitate future clinical applications of QDs.

In this paper, a new  $^{188}\text{Re}$ -labeled RGD (arginine–glycine–aspartic acid) peptide-CdTe QDs dual modality probe was synthesized.  $^{188}\text{Re}$  is an attractive isotope offering potential for targeted radiotherapy of cancer due to its easy availability and suitable nuclear properties ( $E_{\beta\text{max}} = 2.1 \text{ MeV}$ ,  $t_{1/2} = 16.9 \text{ h}$ ) [14]. Furthermore, the associated  $\gamma$ -emission ( $E_{\gamma} = 155 \text{ keV}$ ) makes it suitable for imaging in single photon emission computed tomography (SPECT) [15]. The RGD sequence is currently the basic module for a variety of RGD-containing peptides which display preferential binding to  $\alpha_v\beta_3$  integrin, which plays a key role in tumor angiogenesis and metastasis and were not detectable on normal blood vessels [16]. So, the dual modality probe could noninvasively visualize the integrin  $\alpha_v\beta_3$  expression at the tumor location using optical imaging and carry out targeted radiotherapy of tumor. Moreover, it could accurately assess the tumor-targeting efficacy, biodistribution and therapeutic effect using optical/SPECT imaging, which would overcome the tissue penetration limitation and be potential

\* Corresponding author. Tel.: +86 21 59556884.

E-mail address: [yongxianwangsinap@163.com](mailto:yongxianwangsinap@163.com) (Y. Wang).

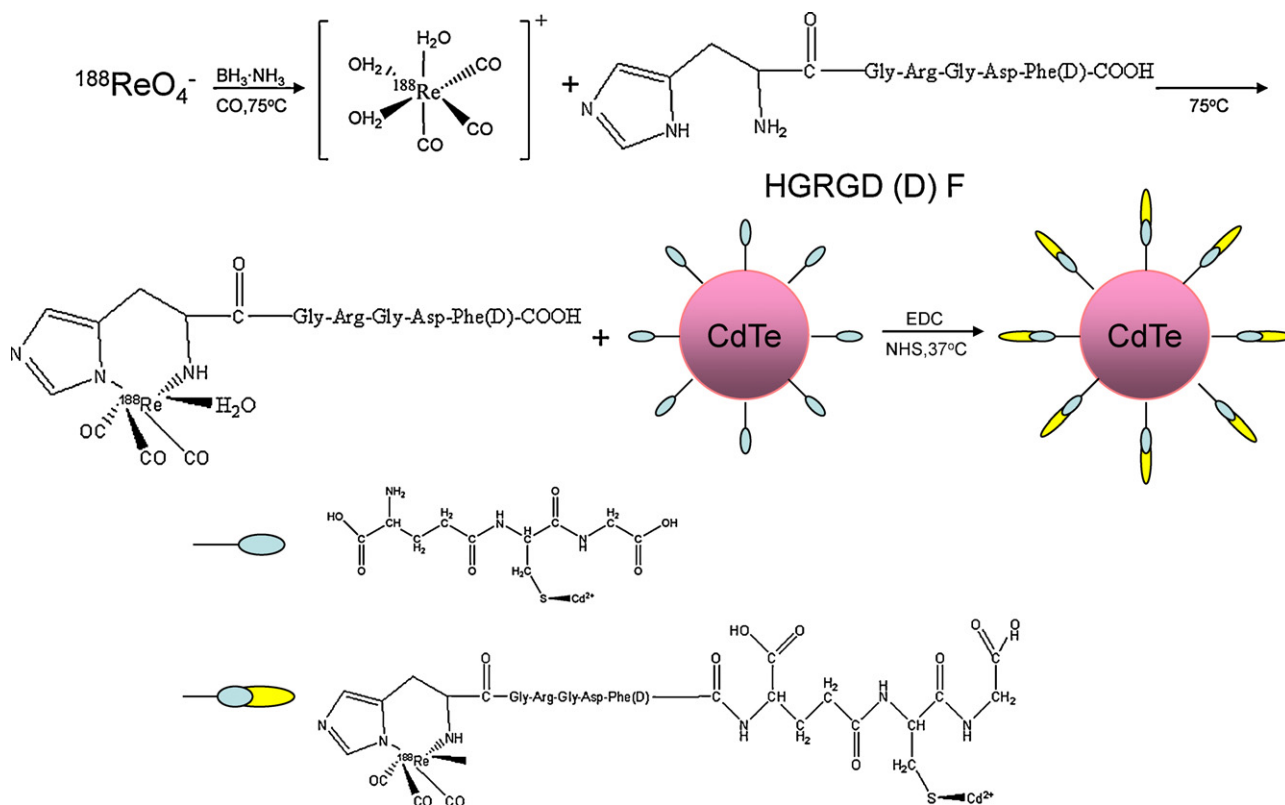


Fig. 1. The radiochemical synthesis of  $^{188}\text{Re}$ -HGRGD (D) F-CdTe QDs.

to accelerate clinical molecular imaging technical progress in future.

## 2. Experimental

### 2.1. Materials and apparatus

Te powder (99.99%); borane ammonia complex ( $\text{BH}_3\cdot\text{NH}_3$ , 97%), 1-[3-(dimethylamino)propyl]-3-ethylcarbodiimide-methiodide (EDC), L-glutathione reduced (GSH, 98%) and N-hydroxysuccinimide (NHS, 98%) were obtained from Sigma–Aldrich.  $\text{NaBH}_4$  (96%), NaOH (AR),  $\text{CdCl}_2\cdot 2.5\text{H}_2\text{O}$  (AR) and  $\text{CH}_3\text{CN}$  (HPLC) were purchased from Sinopharm Chemical Reagent Co., Ltd (China). CO gas was purchased from Shanghai PolyGas Technology Co., Ltd. Carrier-free  $^{188}\text{Re}$ -perrhenate was freshly eluted with saline from an alumina-based  $^{188}\text{W}/^{188}\text{Re}$ -generator (made by Radiopharmaceutical Centre, Shanghai Institute of Applied Physics). HGRGD (D) F (95%) was synthesized by Shanghai AmbioPharm, Inc. All other chemicals and materials were of analytical grade.

$\lambda$ -Counter (SN-697, Shanghai Rihuan Photoelectronic Instrument Co., Ltd.), radio-thin layer chromatography (AR2000, Bioscan) and high-performance liquid chromatography (with PDA-100 UV/Vis detector and Flow-Count TM radioactivity detector, Bioscan) were used for radioactivity analysis. Fluorescence spectra were achieved with a Hitachi F-4500 FL spectrophotometer. The images of cells were taken on ZEISS Axioskop2 fluorescence microscope.

### 2.2. Preparation of GSH-CdTe QDs

$\text{NaTe}$  solution, prepared from Te powder and  $\text{NaBH}_4$ , was added to  $\text{N}_2$ -saturated  $\text{CdCl}_2$  solution in the presence of GSH. The molar ratio of  $\text{Cd}^{2+}:\text{Te}^{2-}:\text{GSH}$  was fixed at 1.0:0.5:2.0. Then, the

solution was adjusted to pH 9.0–9.5 with 1 M NaOH solution. After mixing, the reaction solution was heated to  $100^\circ\text{C}$  and refluxed for 2 h to prepare GSH-capped CdTe QDs. Finally, it was precipitated with isopropyl alcohol, isolated and redissolved in PBS solution.

### 2.3. Synthesis of $\text{fac}-[^{188}\text{Re}(\text{CO})_3(\text{H}_2\text{O})_3]^+$

0.0050 g of  $\text{BH}_3\cdot\text{NH}_3$  was added to cylindriod vial. Then it was stamped, sealed and flushed with CO. 1 ml of  $^{188}\text{ReO}_4^-$  (dissolved in saline, 9.3–18.5 MBq) and 8  $\mu\text{l}$  of concentrated phosphoric acid were injected into the vial, which was immediately heated to  $75^\circ\text{C}$  for 15 min to prepare  $\text{fac}-[^{188}\text{Re}(\text{CO})_3(\text{H}_2\text{O})_3]^+$ . Finally, it was purified using sep-pak QMA cartridge. The radiochemical purity of  $\text{fac}-[^{188}\text{Re}(\text{CO})_3(\text{H}_2\text{O})_3]^+$  was determined by radio-TLC, using a Silica GF254 glass plate with  $\text{CH}_3\text{OH}:\text{HCl}$  (36%) [17].

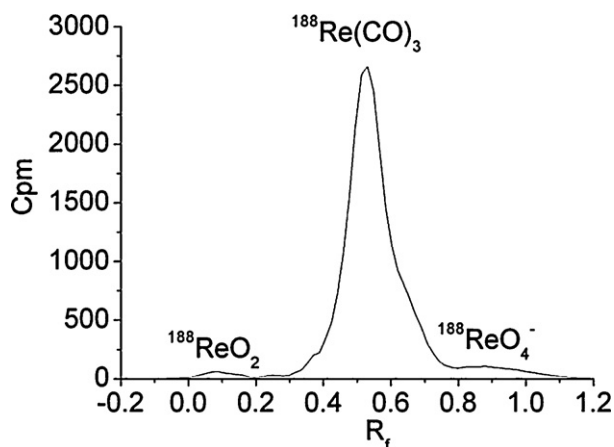
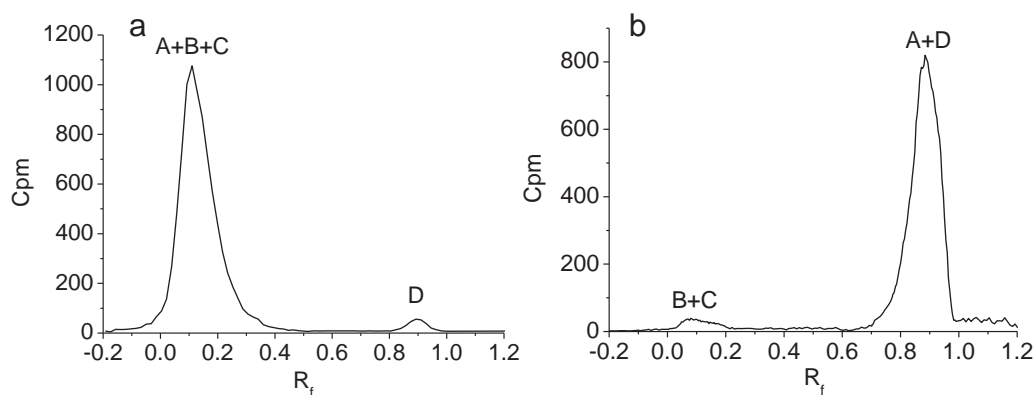


Fig. 2. The radio-TLC of  $\text{fac}-[^{188}\text{Re}(\text{CO})_3(\text{H}_2\text{O})_3]^+$ .



**Fig. 3.** The radiolabeled peptide was analyzed using radio-TLC systems with two different mobile phases: (a)  $\text{CH}_3\text{CN}$  (100%), (b)  $\text{CH}_3\text{COCH}_3/\text{H}_2\text{O}$  (1/1). A, B, C and D stand for  $^{188}\text{Re}$ -HGRGD (D) F, unreacted  $\text{fac-}[^{188}\text{Re}(\text{CO})_3(\text{H}_2\text{O})_3]^+$ ,  $^{188}\text{ReO}_2$  and  $^{188}\text{ReO}_4^-$ , respectively.

#### 2.4. Radiochemical synthesis of $^{188}\text{Re}$ -HGRGD (D) F

A solution of 450  $\mu\text{l}$  of  $\text{fac-}[^{188}\text{Re}(\text{CO})_3(\text{H}_2\text{O})_3]^+$  (3.7–7.4 MBq) in saline was added to the HGRGD (D) F solution (4 mg/ml, 50  $\mu\text{l}$ ). The reaction mixture was stirred at 75  $^\circ\text{C}$  for 30 min and then cooled in an ice bath. Radio-TLC and -HPLC were used to control the identity, radiochemical purity, and stability of the preparations. For TLC studies, silica gel strips (GF254) were used and developed with either  $\text{CH}_3\text{COCH}_3/\text{H}_2\text{O}$  (1/1) or  $\text{CH}_3\text{CN}$  (100%). The HPLC analyses were carried out with a reverse-phase C18 column using a gradient eluant of  $\text{H}_2\text{O}$  (A) with 0.1%  $\text{CF}_3\text{COOH}$  and  $\text{CH}_3\text{CN}$  (B) with 0.1%  $\text{CF}_3\text{COOH}$ , gradient elution: 0–30 min 5% B, 30–35 min 60% B,

35–40 min 5% B and a flow rate of 1.0 ml/min. To purify the product, the desired fraction of  $^{188}\text{Re}$ -HGRGD (D) F was collected from HPLC, and then it was concentrated and evaporated under reduced pressure. Finally, the purified product was redissolved in PBS solution.

#### 2.5. Conjugation of $^{188}\text{Re}$ -HGRGD (D) F-CdTe QDs

To a mixture of 500  $\mu\text{l}$  of  $^{188}\text{Re}$ -HGRGD (D) F and 500  $\mu\text{l}$  of CdTe QDs, we added 50  $\mu\text{l}$  of EDC (0.1 mol/L) and 10  $\mu\text{l}$  of NHS (0.1 mol/L). The mixture was incubated for 12 h and the uncoupled free  $^{188}\text{Re}$ -HGRGD (D) F was removed by precipitation, centrifuga-

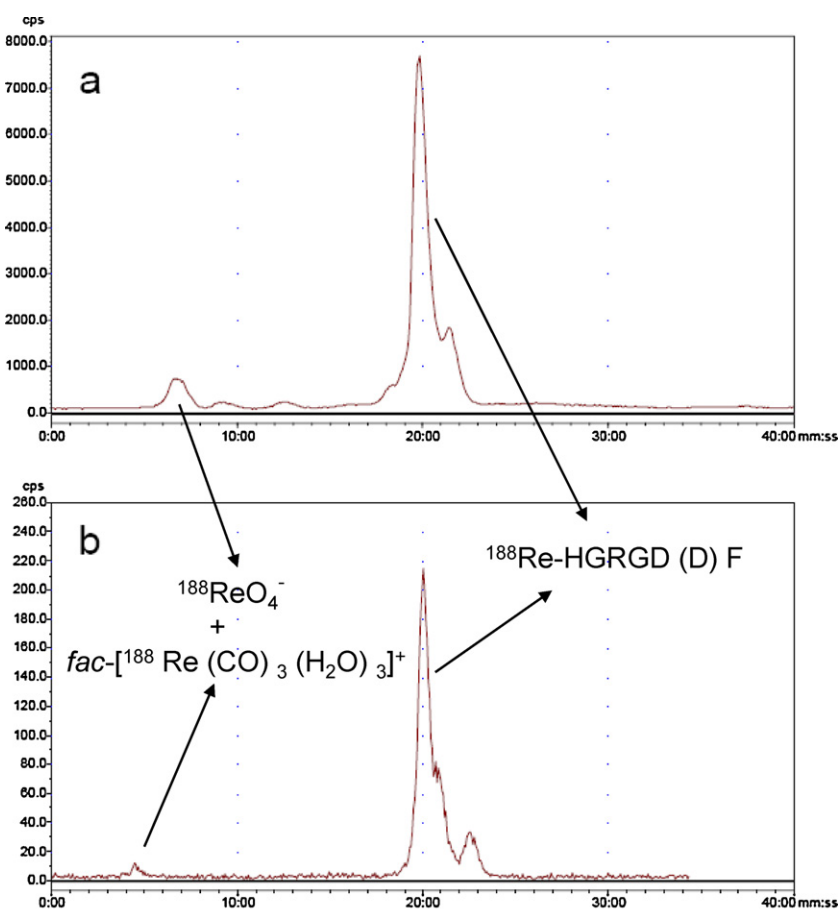


**Fig. 4.** HPLC-radiochromatogram of  $^{188}\text{Re}$ -HGRGD (D) F. (a) Without purification; (b) with purification.

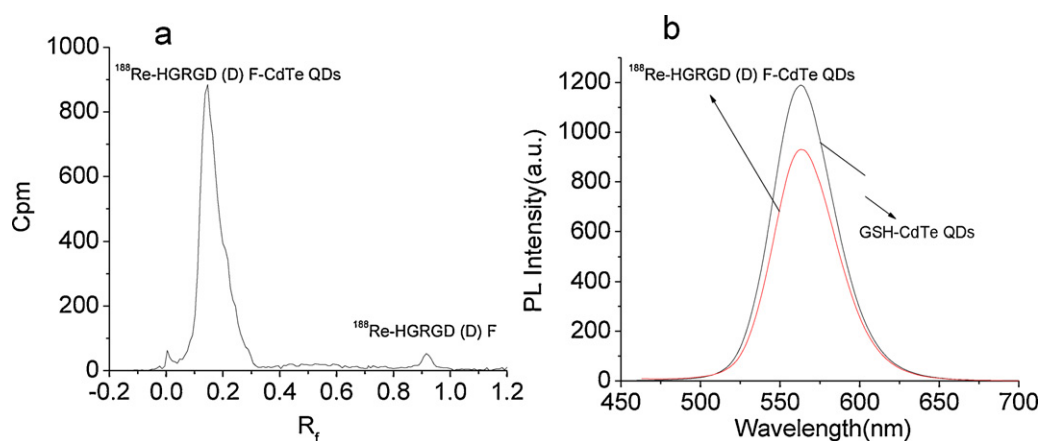


Fig. 5. TLC-radiochromatogram (a) and PL spectra (b) of  $^{188}\text{Re}$ -HGRGD (D) F-CdTe QDs.  $\lambda_{\text{ex}} = 440 \text{ nm}$ .

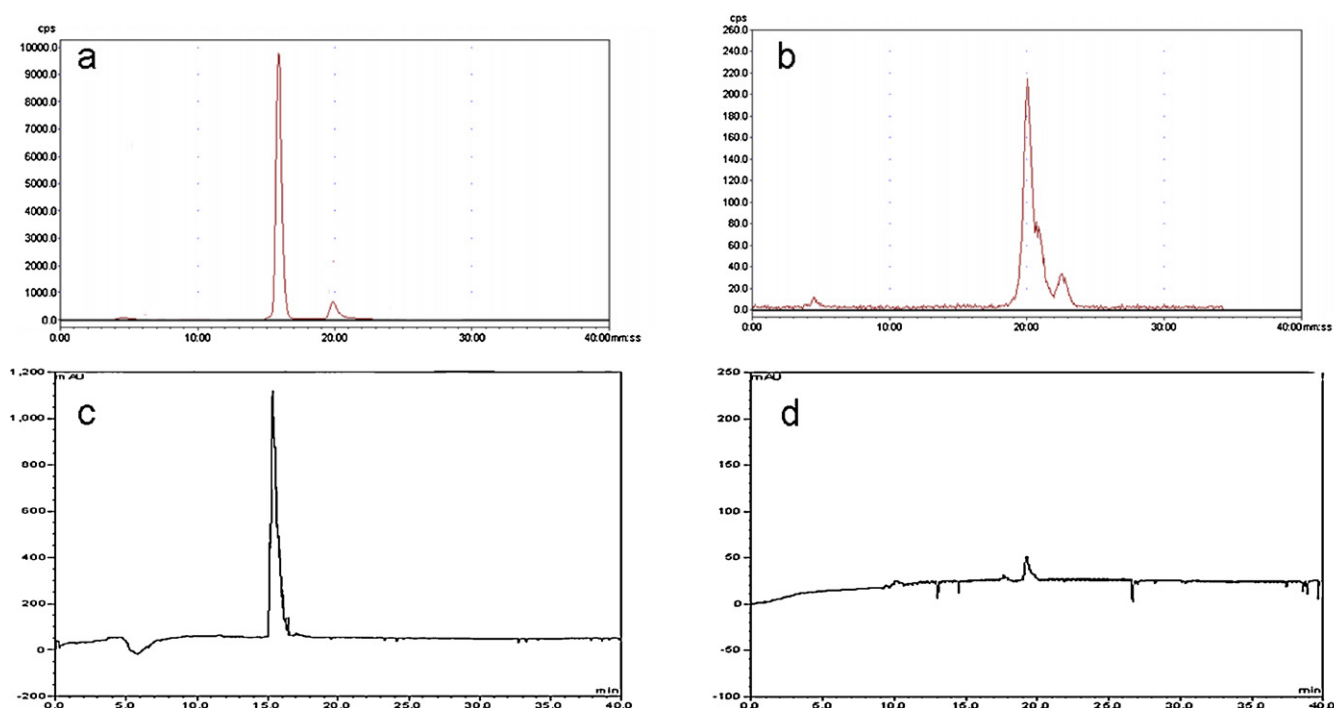


Fig. 6. HPLC chromatogram analysis of  $^{188}\text{Re}$ -HGRGD (D) F-QDs (a, c) and  $^{188}\text{Re}$ -HGRGD (D) F (b, d). The figures shown in (c) and (d) were both monitored by a UV-vis detector at 400 nm.

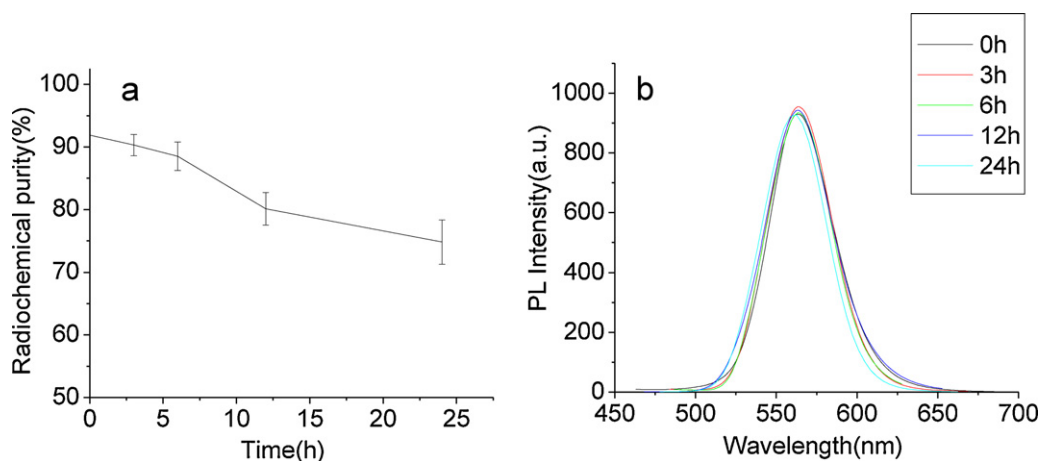


Fig. 7. In vitro stability of  $^{188}\text{Re}$ -HGRGD (D) F-CdTe QDs. (a) Radiochemical purity; (b) PL spectra.

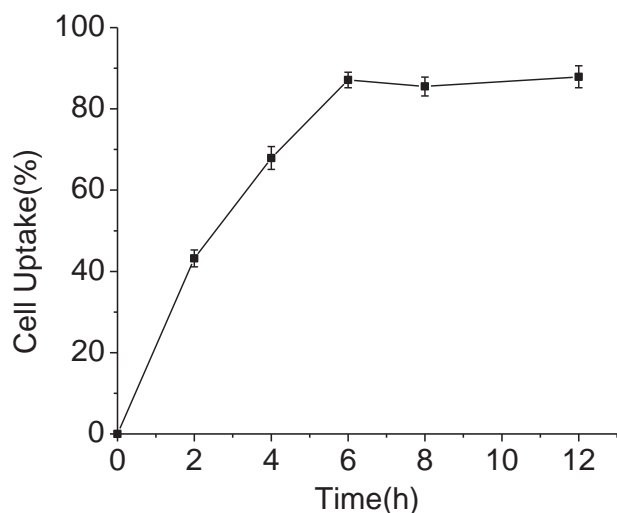


Fig. 8. The cell uptake ratio of  $^{188}\text{Re}$ -HGRGD (D) F-CdTe QDs.

gation and isolation. The final complex was redissolved in PBS or DMEM solution and kept at 4 °C.

## 2.6. In vitro stability studies

A solution of 500  $\mu\text{l}$  of  $^{188}\text{Re}$ -HGRGD (D) F-CdTe QDs (1.0–2.0 MBq) was mixed with 500  $\mu\text{l}$  of NCF and incubated at 37 °C. The solution was analyzed at intervals of 3, 6, 12 and 24 h by TLC analyses using silica gel strips with  $\text{CH}_3\text{COCH}_3/\text{H}_2\text{O}$  (1/1) and HPLC analyses using a gradient eluant of  $\text{H}_2\text{O}$  (A) with 0.1%  $\text{CF}_3\text{COOH}/\text{CH}_3\text{CN}$  (B) with 0.1%  $\text{CF}_3\text{COOH}$ , gradient elution: 0–30 min 5% B, 30–35 min 60% B, 35–40 min 5% B and a flow rate of 1.0 ml/min.

## 2.7. In vitro cell binding assays

Human glioblastoma U87MG cells, known to express  $\alpha_v\beta_3$  integrin, were cultured at 37 °C, in 5%  $\text{CO}_2$  in DMEM, supplemented with 10% heat-inactivated newborn calf serum (NCF). The cells were plated into a 96-well plate at  $1.2 \times 10^4$  cells/well (200  $\mu\text{l}$ /well). After 24-h incubation, the DMEM was removed. Then they were incubated with 200  $\mu\text{l}$  of  $^{188}\text{Re}$ -HGRGD (D) F-CdTe QDs (in DMEM, 20  $\mu\text{g}/\text{ml}$ , 0.037 MBq/well) at 37 °C for different times, respectively. At the end of incubation, cells were washed twice with 200  $\mu\text{l}$  of PBS and underwent measurement of radioactivity on high-energy gamma counter along with standards and fluorescence microscope.

## 3. Results and discussion

### 3.1. Chemical and radiochemical synthesis

$\text{fac-}[^{188}\text{Re}(\text{CO})_3(\text{H}_2\text{O})_3]^+$ , which could be readily generated from  $^{188}\text{ReO}_4^-$  and CO gas in the presence of  $\text{BH}_3\text{-NH}_3$  [18], is an attractive core for the introduction of  $^{188}\text{Re}$  into biomolecules because of its high chemical stability and small size. As shown in Fig. 1, after  $\text{fac-}[^{188}\text{Re}(\text{CO})_3(\text{H}_2\text{O})_3]^+$  was synthesized, HGRGD (D) F could be labeled with  $^{188}\text{Re}$  by the chelating reaction of  $\text{fac-}[^{188}\text{Re}(\text{CO})_3(\text{H}_2\text{O})_3]^+$  and HGRGD (D) F. Finally, the  $^{188}\text{Re}$ -HGRGD (D) F-CdTe QDs conjugate was prepared through the amidation reaction between  $-\text{NH}_2$  on the surface of QDs and  $-\text{COOH}$  on the surface of  $^{188}\text{Re}$ -HGRGD (D) F in the presence of EDC and NHS. The TLC chromatography of  $\text{fac-}[^{188}\text{Re}(\text{CO})_3(\text{H}_2\text{O})_3]^+$  after purification is shown in Fig. 2. In this system, colloidal

$^{188}\text{ReO}_2$ , formed due to over-reduction of  $^{188}\text{ReO}_4^-$ , stayed near the origin ( $R_f=0$ ), the  $R_f$  of  $\text{fac-}[^{188}\text{Re}(\text{CO})_3(\text{H}_2\text{O})_3]^+$  was 0.4–0.6, and the unreacted  $^{188}\text{ReO}_4^-$  had an  $R_f$  of 0.8–1.0. The radiochemical purity of  $\text{fac-}[^{188}\text{Re}(\text{CO})_3(\text{H}_2\text{O})_3]^+$  was above 93% analyzed by TLC. After Labeling of HGRGD (D) F with  $\text{fac-}[^{188}\text{Re}(\text{CO})_3(\text{H}_2\text{O})_3]^+$ , the radioactive products included  $^{188}\text{Re}$ -HGRGD (D) F, unreacted  $\text{fac-}[^{188}\text{Re}(\text{CO})_3(\text{H}_2\text{O})_3]^+$ , a small quantity of  $^{188}\text{ReO}_2$  and  $^{188}\text{ReO}_4^-$  formed during the synthesis of  $\text{fac-}[^{188}\text{Re}(\text{CO})_3(\text{H}_2\text{O})_3]^+$ . As shown in Fig. 3, they would show different  $R_f$  values by TLC with  $\text{CH}_3\text{COCH}_3/\text{H}_2\text{O}$  (1/1) or  $\text{CH}_3\text{CN}$  (100%). So, it is feasible to calculate the labeling efficiency according to Eq. (1) or (2):

$$A\% = (A + B + C)\% - (B + D)\% \quad (1)$$

$$A\% = (A + D)\% - (D)\% \quad (2)$$

here A%, B%, C% and D% are percentage of corresponding integral area in TLC, respectively. The result showed the  $^{188}\text{Re}$  labeling efficiency of HGRGD (D) F was above 90%.

In order to remove  $^{188}\text{ReO}_2$ ,  $^{188}\text{ReO}_4^-$  and unreacted  $\text{fac-}[^{188}\text{Re}(\text{CO})_3(\text{H}_2\text{O})_3]^+$ , the labeling products were purified by HPLC. As can be observed in Fig. 4, the purity of  $^{188}\text{Re}$ -HGRGD (D) F ( $t_R=20$  min) could be improved from 90.7% to 96.2% (calculated by corresponding integral area) after purification. Then, the purified  $^{188}\text{Re}$ -HGRGD (D) F was used to prepare the  $^{188}\text{Re}$ -HGRGD (D) F-CdTe QDs conjugates. Once the  $^{188}\text{Re}$ -HGRGD (D) F-CdTe QDs conjugate formed, it would produce different developing effect by TLC compared with  $^{188}\text{Re}$ -HGRGD (D) F due to different particle sizes and polarity. As shown in Fig. 5a, when developed using silica gel strips (GF254) as stationary phase with  $\text{CH}_3\text{COCH}_3/\text{H}_2\text{O}$  (1/1), the  $^{188}\text{Re}$ -HGRGD (D) F-CdTe QDs remained at the origin ( $R_f=0$ ) because of its larger particle size and unreacted  $^{188}\text{Re}$ -HGRGD (D) F traveled with the solvent front with a  $R_f$  value of 0.8–1.0. It was found the radiochemistry yield of  $^{188}\text{Re}$ -HGRGD (D) F-CdTe QDs was about 92.1% by calculating corresponding integral area in TLC chromatography. Furthermore, the photoluminescence (PL) emission spectra of  $^{188}\text{Re}$ -HGRGD (D) F-CdTe QDs were examined, too. As shown in Fig. 5b, the emission peak position of QDs had no obvious change basically after conjugated with  $^{188}\text{Re}$ -HGRGD (D) F, although the PL intensity would decrease lightly. For further proving the formation of  $^{188}\text{Re}$ -HGRGD (D) F-CdTe QDs conjugate, the sample was analyzed by HPLC chromatogram, which is shown in Fig. 6. Compared with  $^{188}\text{Re}$ -HGRGD (D) F, the strongest radioactive peak would move from 20 min to 16 min. Moreover, there were still two weak peaks at 20 min and 5 min. After  $^{188}\text{Re}$ -HGRGD (D) F was linked with QDs, the  $t_R$  would become shorter due to the larger sizes and weaker interaction with reverse-phase C18 column of  $^{188}\text{Re}$ -HGRGD (D) F-CdTe QDs [19,20]. So, we concluded that the radioactive substances, whose  $t_R$  were at the positions of 5 min, 16 min and 20 min, were  $\text{fac-}[^{188}\text{Re}(\text{CO})_3(\text{H}_2\text{O})_3]^+$ ,  $^{188}\text{Re}$ -HGRGD (D) F-CdTe QDs and unreacted  $^{188}\text{Re}$ -HGRGD (D) F, respectively. In addition, the product was analyzed by UV detectors in HPLC. As shown in Fig. 6, there was a weak adsorption peak at the peak time of  $^{188}\text{Re}$ -HGRGD (D) F, proving  $^{188}\text{Re}$ -HGRGD (D) F had only weak UV adsorption. However, there was a strong adsorption at the peak time of  $^{188}\text{Re}$ -HGRGD (D) F-CdTe QDs, which was caused by QDs basically. So, it was certain that  $^{188}\text{Re}$ -HGRGD (D) F was linked with QDs successfully and the peak time of  $^{188}\text{Re}$ -HGRGD (D) F-CdTe QDs conjugate would move forward to 16 min.

### 3.2. In vitro stability

To study the *in vitro* stability of  $^{188}\text{Re}$ -HGRGD (D) F-QDs, the radiochemical purity of  $^{188}\text{Re}$ -HGRGD (D) F-QDs was exam-

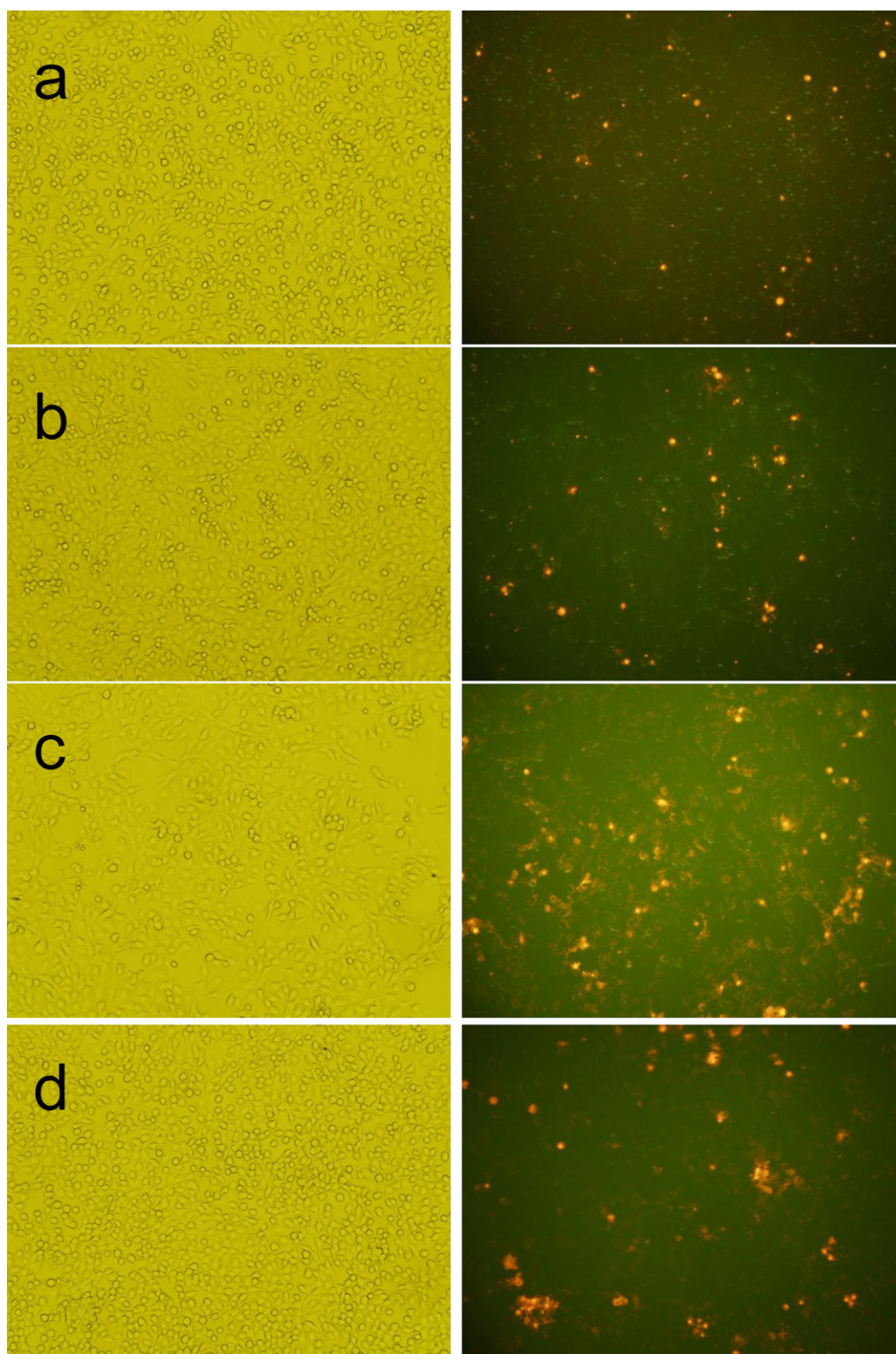


**Fig. 9.** Fluorescence images of U87MG cells after incubation with  $^{188}\text{Re}$ -HGRGD (D) F-CdTe QDs. a: 2 h; b: 4 h; c: 6 h; d: 8 h. Left: bright field; right: fluorescence.

ined by radio-TLC and HPLC analysis after incubation with NCF at  $37^\circ\text{C}$  (Fig. 7a). As shown, the radiochemical purity of  $^{188}\text{Re}$ -HGRGD (D) F-QDs was 90.3%, 88.5%, 80.1% and 74.8% for 3, 6, 12 and 24 h, respectively. So, it was not very stable after incubation with NCF solution for a long time. We speculated that some functional protein existing in NCF could lead to hydrolysis of amidation bond in  $^{188}\text{Re}$ -HGRGD (D) F-QDs. Besides, the

probable bond of  $^{188}\text{Re}$ -HGRGD (D) F-QDs with protein would change the polarity in TLC and HPLC analysis. A further research is needed to find the exact reason. In addition, the PL stability was investigated, too. As shown in Fig. 7b, the PL peak position and intensity had no obvious change basically, which would show the strong stability of CdTe QDs in NCF solution.

### 3.3. Cellular uptake

The problem of effective quantitative analysis of fluorescence signal could be solved using radioactivity determination. So, it could accelerate the application of QDs-based probe in the field of biological medicine greatly. To evaluate the cellular uptake of  $^{188}\text{Re}$ -HGRGD (D) F-CdTe QDs, U87MG cells were cultured in DMEM culture medium containing  $^{188}\text{Re}$ -HGRGD (D) F-CdTe QDs. Then, the culture medium was removed, and radioactivity was measured to estimate the quantity of  $^{188}\text{Re}$ -HGRGD (D) F-CdTe QDs entering into U87MG cells. As shown in Fig. 8, the uptake ratio of  $^{188}\text{Re}$ -HGRGD (D) F-CdTe QDs would increase gradually as incubation continued, indicating  $^{188}\text{Re}$ -HGRGD (D) F-CdTe QDs entered into cells gradually. The uptake ratio could reach 87.3% after incubation for 6 h; however the uptake ratio almost had no increase with further incubation, which indicated a part of radioactivity could not get into the cells. It would be caused by the decomposition of  $^{188}\text{Re}$ -HGRGD (D) F-CdTe QDs in DMEM culture medium. Furthermore, the aggregation of QDs in DMEM would increase its sizes and make negative impact to cellular uptake. The fluorescence microscope images of U87MG cells incubating with  $^{188}\text{Re}$ -HGRGD (D) F-CdTe QDs for different times were analyzed, too. The results are shown in Fig. 9. Be similar with the analysis of radioactivity, the PL intensity increased gradually as incubation continued, proving that CdTe QDs had been combined with  $^{188}\text{Re}$ -HGRGD (D) F successfully and entered into cells through the targeting of HGRGD (D) F.

### 4. Conclusions

In summary, a new  $^{188}\text{Re}$ -HGRGD (D) F-CdTe QDs dualmodality probe was synthesized. It could detect the tumor location with fluorescence imaging and assess the tumor-targeting efficacy of probe with radioactive analysis. We believe this study would provide encouraging support for the future development of QDs-based probe. To prove its application value in clinical medicine, a further effort should be made to indicate the biodistribution and biotoxicity of this dualmodality probe. Besides, the radiotherapy effect of  $^{188}\text{Re}$  in this probe should be further studied and thus performs the function of both therapy and imaging successfully.

### Acknowledgements

The authors gratefully acknowledge the financial support from the National Natural Science Foundation of China (Nos. 10805069 and 10405034).

### References

- [1] N. Gaponik, D.V. Talapin, A.L. Rogach, K. Hoppe, E.V. Shevchenko, A. Kornowski, A. Eychmüller, H. Weller, *J. Phys. Chem. B* 106 (2002) 7177.
- [2] Y.C. Kuo, Q. Wang, C. Ruengruglikit, H.L. Yu, Q.R. Huang, *J. Phys. Chem. C* 112 (2008) 4818.
- [3] J. Ma, Q. Fan, L. Wang, N. Jia, Z. Gub, H. Shena, *Talanta* 81 (2010) 1162.
- [4] L.D. Chen, J. Liu, X.F. Yu, M. He, X.F. Pei, Z.Y. Tang, Q.Q. Wang, D.W. Pang, Y. Li, *Biomaterials* 29 (2008) 4170.
- [5] X. Gao, Y. Cui, R.M. Levenson, L.W.K. Chung, S. Nie, *Nat. Biotechnol.* 22 (2004) 969.
- [6] M.K. So, C. Xu, A.M. Loening, S.S. Gambhir, J. Rao, *Nat. Biotechnol.* 24 (2006) 339.
- [7] X. Montet, J.L. Figueiredo, H. Alencar, V. Ntziachristos, U. Mahmood, R. Weissleder, *Radiology* 242 (2007) 751.
- [8] V. Ntziachristos, C.H. Tung, C. Bremer, R. Weissleder, *Nat. Med.* 8 (2002) 757.
- [9] L. Prinzen, R.-J.J.H.M. Mijer, A. Dirksen, T.M. Hackeng, N. Deckers, N.J. Bitsch, R.T.A. Megens, K. Douma, J.W. Heemskerk, M.E. Kooi, P.M. Frederik, D.W. Slaaf, M.A.M.J. van Zandvoort, C.P.M. Reutelingsperger, *Nano Lett.* 7 (2007) 93.
- [10] S.Z. Wang, B.R. Jarrett, S.M. Kauzlarich, A.Y. Louie, *J. Am. Chem. Soc.* 129 (2007) 3848.
- [11] M.L. Schipper, Z. Cheng, S.W. Lee, L.A. Bentolila, G. Iyer, J. Rao, X. Chen, A.M. Wu, S. Weiss, S.S. Gambhir, *J. Nucl. Med.* 48 (2007) 1511.
- [12] M.L. Schipper, G. Iyer, A.L. Koh, Z. Cheng, Y. Ebenstein, A. Aharoni, S. Keren, L.A. Bentolila, J. Li, J. Rao, X. Chen, U. Banin, A.M. Wu, R. Sinclair, S. Weiss, S.S. Gambhir, *Small* 5 (2009) 126–134.
- [13] F. Ducongé, T. Pons, C. Pestourie, L. Hérin, B. Thézé, K. Gombert, B. Mahler, F. Hinnen, B. Kühnast, F. Dollé, B. Dubertret, B. Tavitian, *Bioconjug. Chem.* 19 (2008) 1921.
- [14] N. Iznaga-Escobar, *Nucl. Med. Biol.* 25 (1998) 441.
- [15] L.C. Chen, C.H. Chang, C.Y. Yu, Y.J. Chang, Y.H. Wu, W.C. Lee, C.H. Yeh, T.W. Lee, G. Ting, *Nucl. Med. Biol.* 35 (2008) 883.
- [16] K. Temming, R.M. Schiffelers, G. Molema, R.J. Kok, *Drug Resist. Update* 8 (2005) 381.
- [17] J. Cao, Y. Wang, J. Yu, J. Xia, C. Zhang, D. Yin, U.O. Häfeli, J. Magn. Mater. 277 (2004) 165.
- [18] J. Xia, Y. Wang, J. Yu, J. Cao, C.u. Zhang, D. Yin, *J. Radioanal. Nucl. Chem.* 266 (2005) 313.
- [19] G. Iyer, F. Pinaud, J. Tsay, J.J. Li, L.A. Bentolila, X. Michalet, S. Weiss, *IEEE Trans. Nanobiosci.* 5 (2006) 231.
- [20] D.K. Tiwari, S.I. Tanaka, Y. Inouye, K. Yoshizawa, T.M. Watanabe, T. Jin, *Sensors* 9 (2009) 9332.